

# Influence of the Porous Morphology on the *In Vitro* Degradation and Mechanical Properties of Poly(L-lactide) Disks

Pierre Sarazin, Nick Virgilio, Basil D. Favis

CREPEC, Department of Chemical Engineering, École Polytechnique de Montréal, Montréal, Quebec H3C 3A7, Canada

Received 18 June 2004; accepted 10 June 2005

DOI 10.1002/app.23185

Published online in Wiley InterScience (www.interscience.wiley.com).

**ABSTRACT:** Poly(L-lactide) (PLLA) materials having an interconnected porosity are proposed as an alternative to nonporous biomaterials. Such materials allow for the potential of modulating the degradation behavior and the mechanical properties. In this article, the preparation of porous PLLA disks or cylinders with 50 and 65% void volume is presented. It is demonstrated that both a symmetric and asymmetric porosity can be generated within the disk itself. In addition, open- and closed-cell structures can also be prepared. The accelerated *in vitro* degradation on symmetric open-cell porous PLLA disks and on the nonporous control indicate a similar behavior in terms of melting temperature and inherent viscosity of the remaining pieces of the speci-

mens, but the crystallinity and the mass of the remaining fragments are much smaller for the porous specimens. The mechanical properties under compression are determined for open and closed-cell porous cylinders, porous tubes, and for the nonporous PLLA. The results highlight the excellent mechanical integrity of the prepared porous structures and demonstrate that such materials could have potential for use as biomedical implants. © 2006 Wiley Periodicals, Inc. *J Appl Polym Sci* 100: 1039–1047, 2006

**Key words:** polylactide; macroporous; co-continuity; blends; melt mixing

## INTRODUCTION

Bioabsorbable polymers are making impressive inroads as an alternative to nonresorbable implants. They are generally composed of aliphatic polyesters such as polylactide, polyglycolides, polycaprolactones, and their statistical or block copolymers. Currently, the homopolymers or copolymers of glycolide and lactide have been cleared by the U.S. Food and Drug Administration (FDA).<sup>1</sup> Porous polymer materials have been promoted as carriers or scaffolds for repairing tissues, delivering drugs and bioactives, encapsulating cells, or bioengineering artificial tissues. Ultimately, the biodegradable matrix is entirely replaced by a natural extracellular matrix.<sup>2</sup>

Another important biomedical application of biodegradable polymers is as implants and devices, for example for fracture repairs.<sup>3</sup> The incorporation of bioactive calcium phosphate into a polylactide matrix is also used to improve the mechanical and osteoconductive properties.<sup>4,5</sup> However, long-term experimental studies indicate that poly(L-lactide) (PLLA) has a considerably longer degradation time, up to several

years instead of months.<sup>6–8</sup> Moreover, it is advantageous to minimize the quantity of polymer used to reduce the chance of severe foreign body responses after implantation. The degradation pathway for a given polymer depends on several characteristics: molecular weight, crystallinity, thermal history, geometry, and environment of the implant. A compromise is necessary to obtain adequate mechanical properties and satisfactory degradation.

In a previous work from this laboratory, binary and compatibilized PLLA/polystyrene blends (PS) prepared by melt mixing were examined.<sup>9,10</sup> The onset of the region of co-continuity of the phases was determined at 40–45% PS. It was demonstrated that highly percolated blends of the above materials exist from 40 to 75% PS and 40–60% PS for the binary and compatibilized blends, respectively. Extraction of the PS phase in the blend by selective solvent dissolution left a completely interconnected porosity of highly controlled morphologies (pore size, void volume) in PLLA. This continuous porosity inside the PLLA materials (pore size of about 1–2  $\mu\text{m}$ ) can be used to reduce the quantity of polymer in the final piece, to increase the contact surface area of the polymer with the environment of degradation.

In this article, the preparation of porous PLLA disks is proposed. The mechanical properties in compression and the accelerated *in vitro* degradation are com-

Correspondence to: B. D. Favis (basil.favis@polymtl.ca).

Contract grant sponsor: Natural Sciences and Engineering Research Council of Canada (NSERC).

TABLE I  
Characteristic Properties of Materials

|                                     | PLLA                 | PS      |
|-------------------------------------|----------------------|---------|
| $M_w$                               | —                    | 192,000 |
| Intrinsic viscosity (dL/g)          | 4.1                  | —       |
| Density (20°C) (g/cm <sup>3</sup> ) | 1.27                 | 1.04    |
| Glass temperature (°C)              | 55                   | 105     |
| Melting point (°C)                  | 183                  |         |
| Supplier                            | Boehringer Ingelheim | Dow     |

pared with the nonporous solid PLLA material. The potential of forming open-cell and closed-cell structures as well as symmetric and asymmetric pore morphologies is also examined.

## METHODS

### Materials

A polystyrene (PS) from Dow and a poly(L-lactide) (PLLA) from Boehringer–Ingelheim were used in pellet and powder form, respectively. Some of the characteristics of the resins used are reported in Table I.

### Preparation of the samples

Blends were prepared by melt mixing in a Haake internal mixer as described previously.<sup>10</sup> The mixing blades were maintained at 50 rpm and the temperature was set at 200°C. Time of mixing was 7 min. All the blend concentrations are reported as volume fraction. Two geometries of samples (discs and cylinders) were made by using different processes. Samples of 35% PLLA/65% PS and 100% PLLA were ground mechanically to give a powder, and then pressed at 200°C for 6 min in a compression molding press. A 5-mm diameter disk-like mold of 3 mm thickness was used. During compression, the mold is sandwiched between two steel plates covered by PTFE sheets. After the molding step, the mold was cooled under a cold compression press for 5 min. The polystyrene phase (PS) was then extracted from the molded disks by selective extraction in cyclohexane.

Cylindrical specimens (diameter: 3 mm; height: 5 mm) were fabricated using a circular saw at high speed directly after the mixing step, for solid PLLA and the 50% PLLA/50% PS blend. Tubes were obtained using the same method as for the cylinders. Very few studies have been carried out on macro-tubular PLLA constructs, although it is a desirable shape for many applications. The polystyrene phase was extracted from the cylinders. The cylinders were used for the mechanical tests, while the disks were used for the degradation test.

### Selective solvent extraction of the porogen phase

Extractions were performed in a Soxhlet extraction apparatus. The PS phase was extracted from the disks with cyclohexane, and hence can also be referred to as the porogen phase. The temperature of the cyclohexane in the Soxhlet apparatus was about 50–60°C. After the extraction, the specimens were then dried in a vacuum oven at 50°C. Extraction was performed until the dried extracted specimens achieved constant weight. A gravimetric method was used to calculate the extent of continuity of the PS phase as used previously.<sup>9</sup>

Other specific solvent etching protocols to obtain closed cell and asymmetric porosities are presented in the results and discussion.

### Accelerated *in vitro* degradation on porous PLLA disks

Accelerated hydrolytic *in vitro* degradation studies were performed on porous PLLA materials obtained from injection molding of PLLA/PS 35/65 and on solid PLLA disks. The rate of polymer degradation increases with increasing incubation temperature.<sup>11</sup> The specimens were washed for 48 h in ethanol. Disinfecting in ethanol is a well-established technique, but appears to be unsuitable as a sterilization method because it does not adequately eliminate hydrophilic viruses and bacterial spores.<sup>12</sup> Following our particular protocol of sample preparation, such as melt-processing at high temperature and polymer dissolution, we assume that the use of ethanol is sufficient to sterilize our three-dimensional porous materials. The degradation study in a phosphate-buffered saline solution (PBS) was monitored *in vitro* over a 16-week period. For each data point, two specimens were analyzed. Remaining weight, crystallinity, melting point, and molecular weight via the inherent viscosity were analyzed. Each individual specimen was allowed to degrade in a 50 mL flask loaded with 40 mL potassium PBS (Fisher Scientific B82, pH 7.4 at 37°C) and was placed in a thermostatic oven set at (70 ± 1)°C, following the ISO standard 13781.<sup>13</sup> Porous samples were maintained in the PBS solution because the porosity was not filled by water at the onset of the test.

The remaining weight (RW) was estimated as follows:

$$RW(\%) = 100 \times \frac{W_d}{W_i} \quad (1)$$

$W_i$  being the initial weight of the specimen and  $W_d$  being the weight of the specimen dried after degradation.

The crystallinity and the melting temperature of degraded samples were investigated by DSC (Pyris I,

Perkin–Elmer) calibrated with indium. The samples (5–20 mg) were heated under dry, oxygen-free nitrogen, from 40 to 220°C at a rate of 10°C/min. The degree of crystallinity,  $X_c$ , of the PLLA phase can be calculated as follows:

$$X_c = \frac{\Delta H_m + \Delta H_c}{\Delta H_m^0} \quad (2)$$

where  $\Delta H_m$  and  $\Delta H_c$  designate the measured enthalpy of melting and the measured enthalpy of crystallization, respectively, in Joules per gram (grams of polymer), while  $\Delta H_m^0$  represents the enthalpy for 100% crystalline PLLA. In the text, the values in Joules per gram are used, since various  $\Delta H_m^0$  are reported in the literature between 93 and 135 J/g.<sup>14</sup>

### Microtomy and scanning electron microscopy

After solvent extraction of PS and coating with a gold–palladium alloy, the specimens were observed under a Jeol JSM 840 scanning electron microscope (SEM) at a voltage of 10 kV. To analyze the core of the porous materials, some specimens were microtomed before the extraction step, using a Leica RM 2165 microtome equipped with a glass knife. Closed-cell specimens were cut with a razor blade at the end of the process.

### Intrinsic viscosity measurement

Polymer degradation resulting from processing was evaluated by comparing the intrinsic viscosity of PLLA before and after melt mixing, molding, and after selective dissolution of the PS phase. Intrinsic viscosities were also measured on the fragments from the *in vitro* degradation experiments during 16 weeks. Intrinsic viscosities (in deciliter per gram) were measured in chloroform with an Ubbelohde viscosimeter at 30°C.

### Mercury intrusion porosimetry on porous PLLA

The porosity of the specimens prepared using the earlier protocols was estimated by mercury intrusion porosimetry (MIP), using a Micromeritics Poresizer 9320. The experimental data treatment is based on the Washburn equation.<sup>15</sup>

$$P = - \frac{2\sigma \cos \theta}{r} \quad (3)$$

where  $P$  is the applied pressure,  $r$  the radius of the pore,  $\sigma$  the surface tension of mercury (480 mN/m), and  $\theta$  the contact angle between mercury and polymer (140°). This method provides the number-average di-

ameter, the volume-average diameter, and the pore size distribution.

### Compressive mechanical test

Compressive mechanical properties were measured at room temperature on an Instron 5500R equipped with a 1000 N load cell on the cylindrical specimens from PLLA/PS 50/50 blend and solid PLLA. The specimens were compressed with a crosshead speed of 0.5 mm/min. The modulus was determined with the initial slope of the stress–strain curve and the compressive strength was measured at 10% strain at the onset of the plateau region. Five to eight specimens were tested for each condition.

## RESULTS AND DISCUSSION

### Preparation procedure of the porous materials

PLLA and PS were mixed in the batch mixer at 200°C and 50 rpm for 7 min. The blends were then rapidly quenched in liquid nitrogen. The PLLA/PS 50/50 blend was shaped in cylinders using a circular saw, while 35% PLLA/65% PS blend was ground to a coarse powder (<500  $\mu\text{m}$ ) in a laboratory grinder. After filling the mold with the powder, samples of 100% PLLA and 35% PLLA/65% PS were prepared by melt compression. During this compression step, a small pressure of 0.5 ton was applied progressively to avoid the formation of small air bubbles. Higher pressures tend to deform the structure, forming irregular phase shapes and coarser phases close to the surface. In some cases, high pressures can even result in a skin of solid PLLA at the surface of the disks. In that latter case, the lateral surface was then entirely closed (contact with the steel part of the mold), while the circular surface (contact with the Teflon sheets) had some holes. After molding at low pressure, the PS was then extracted from the scaffold using cyclohexane. This protocol allows for the preparation of porous PLLA with a porosity existing right up to the surface of the disk. After extraction, the porous materials from blend PLLA/PS 35/65 have an average sample weight of  $0.0251 \pm 0.001$  g. Gravimetric analysis of the PS phase in the solvent after the extraction step demonstrates that the continuity of the PS phase is  $(99.3 \pm 0.6)\%$ , indicating that trace amounts of the porogen phase remain in the porous disk. Thus, the void volume is about 65%. Another work from this laboratory studied the case where both components of the blend are biodegradable polymers.<sup>16</sup> This eliminates any problems related to contamination by residual porogen polymers. The intrinsic viscosity  $[\eta]$  of solubilized PLLA was initially 4.1 dL/g. After mixing,  $[\eta]$  declines to 3.7 dL/g.  $[\eta]$  after molding is at 3.2 dL/g. No variation of intrinsic viscosity was observed after the



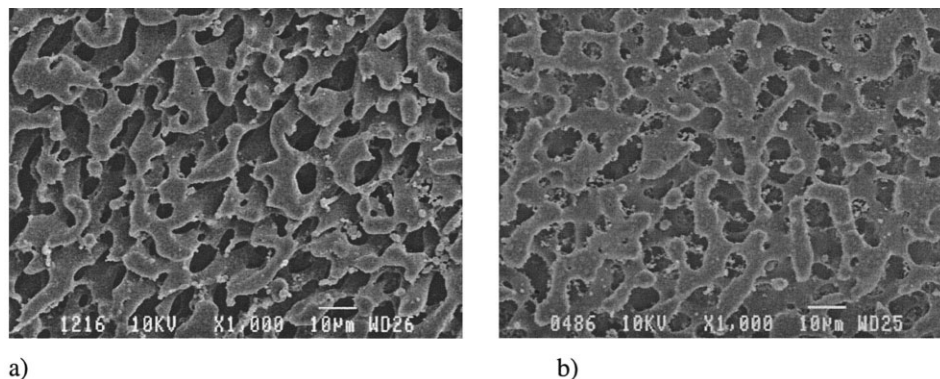


**Figure 1** SEM of PLLA/PS 35/65 blends after selective extraction of the PS phase: (a) from blend in powder form and (b) on a microtomed section of an injection molded disk. The continuity of the PS phase is about 100% for this composition. The white bars indicate 10  $\mu\text{m}$ .

PS extraction process. Figure 1 shows the morphology of the PLLA/PS 35/65 blend after PS extraction on the powder and the injection molded disk. Note that the porosity is continuous inside the material (i.e., interconnected porosity). Figure 2 indicates the corresponding pore size distribution. The PS average volume diameter ( $d_v$ ) increases from 2.9 to 4.1  $\mu\text{m}$  during the molding process.

### Morphology for the porous disks obtained by injection molding

The protocol defined earlier allows for the preparation of porous materials with a symmetric, open-cell porosity. Open-cell morphologies are defined as a state where porosity is maintained right through the material all the way to the surface. A closed-cell morphology is only porous in the core of the scaffold and possesses a solid skin at the surface. A symmetric porous structure can be defined as the case where the

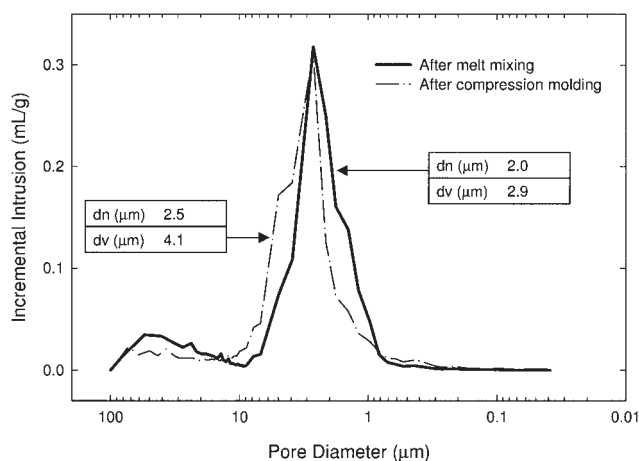


**Figure 2** Pore size distribution as measured by MIP for PLLA porous materials obtained from PLLA/PS 35/65, after melt mixing and after the compression molding step.

porous morphology of the scaffold is identical throughout. An asymmetric porous structure denotes a difference of porous morphology between the bulk and the surface. It will be shown later that variations on the preparation protocol discussed in the previous section can allow for a wide range of porous disk morphologies.

The preparation approach for porous PLLA, derived from a 35% PS/65% PLLA blend, discussed in the previous section, results in a symmetrical open-cell structure. This is clearly shown in Figure 3 where a variety of sections and views are presented. Porosity at the surface is shown in Figure 3(b). Figure 3(c) is a low magnification micrograph, which shows a uniform morphology from the center of the sample right up to the surface. The bulk is shown in Figure 1(b) and the lateral surface is shown in Figure 3(d). The micrographs unambiguously demonstrate the open-cell symmetrical nature of the scaffold.

Asymmetric, open-cell morphologies can be obtained by dissolving the surface of the nonextracted materials for 2 s in chloroform, followed by extraction of the PS phase. The etching in chloroform, a solvent for polylactide, but also for PS, results in large bubble-like pores at the surface of the scaffold (Figs. 4(a) and 4(b)). Note that the structure of the core (not shown here) is identical to the porous morphology shown in Figure 3(c). Increasing the time of etching leads to the formation of some "porous bubbles" and threads of PLLA at the surface.

Closed-cell structures of controlled skin thickness can be obtained by immersing the disks of porous PLLA in chloroform. Figure 4(c) demonstrates a smooth, nonporous external surface. The cross section in Figure 4(d) demonstrates that the internal morphology is porous, with an outer nonporous wall of PLLA of about 40  $\mu\text{m}$  thickness. Increasing the time of immersion in chloroform increases the wall thickness at the surface of the closed-cell disks

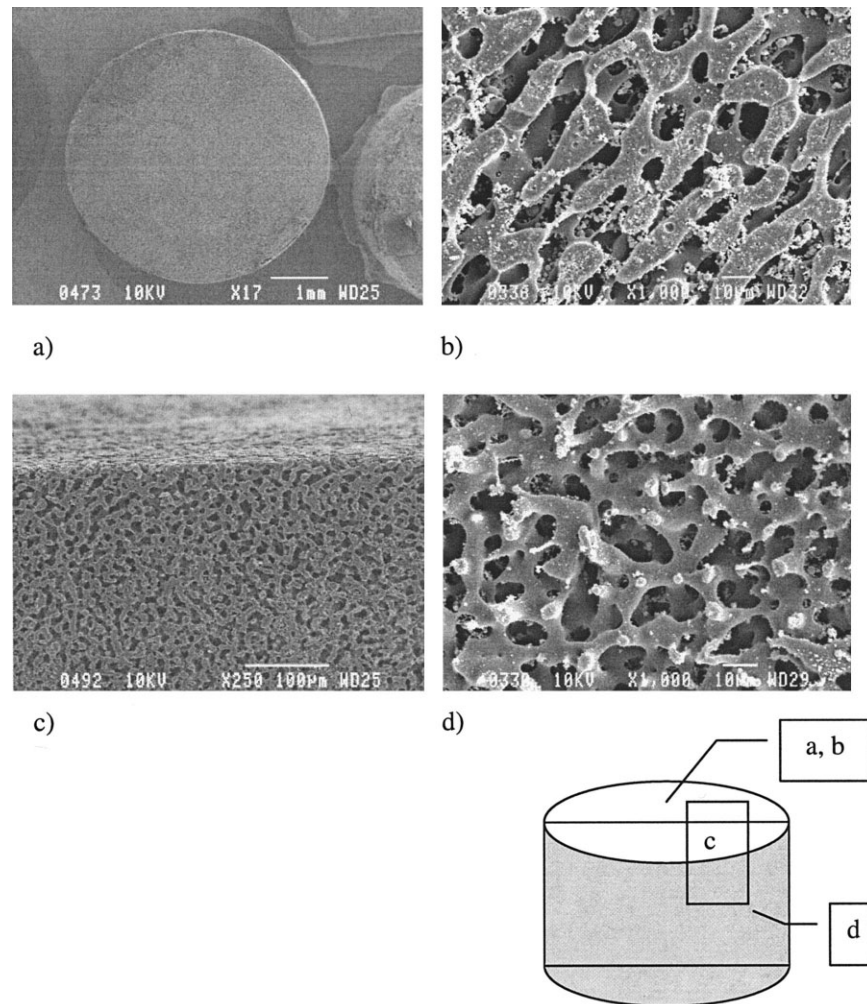


**Figure 3** SEM micrographs of porous PLLA disks with an open-cell symmetric structure (height: 3 mm; diameter: 5 mm) prepared from a PLLA/PS 35/65 blend: (a) top surface of entire disk; (b) top surface of disk, high magnification; (c) view from core to surface; (d) lateral surface of disk.

(and also decreases the diameter of the disks). Skin thickness can thus be closely controlled. Below that skin, the porosity remains highly uniform. This operation results in a porous core and a nonporous skin.

#### Accelerated *in vitro* degradation

Standard accelerated degradation tests at 70°C in a buffer solution were conducted on 65% porous symmetric open-cell PLLA and on nonporous PLLA disks obtained by molding. The inherent viscosity of solubilized PLLA decreased mostly in the first 2 weeks of the experiment to reach 0.5 dL/g (Fig. 5). The thermal properties (the melting temperature,  $T_m$ , and the enthalpy of melting) as a function of accelerated *in vitro* degradation are shown in Figure 6. Only the initial specimens (at  $t = 0$ ) give an exothermic crystallization enthalpy ( $\Delta H_c$ ), resulting from the crystallization phenomenon due to the

reorientation of the amorphous structure during the DSC heat scan before the melting point. We assume that the difference ( $\Delta H_m + \Delta H_c$ ) corresponds to the amount of the original crystallinity. The value of  $T_m$  decreases with increase in hydrolysis time, as usually observed.<sup>14</sup> The enthalpy of melting increases from 30 to 85 J/g with increasing hydrolysis time up until 21–28 days in the same fashion for the two types of samples. Having reached the maximum, the endothermic melting enthalpy peak becomes less and less pronounced with hydrolysis time and decreases more rapidly for the remaining part of the porous PLLA material.

The weight of the specimens is unchanged for the first 2 weeks of the experiment. After 3 weeks, the weight of the dried specimens progressively decreases (Fig. 7) and it appears at that point that the porosity is no longer apparent at the surface of the disk. For a similar inherent viscosity, Figure 7 clearly indicates a more rapid weight loss for the

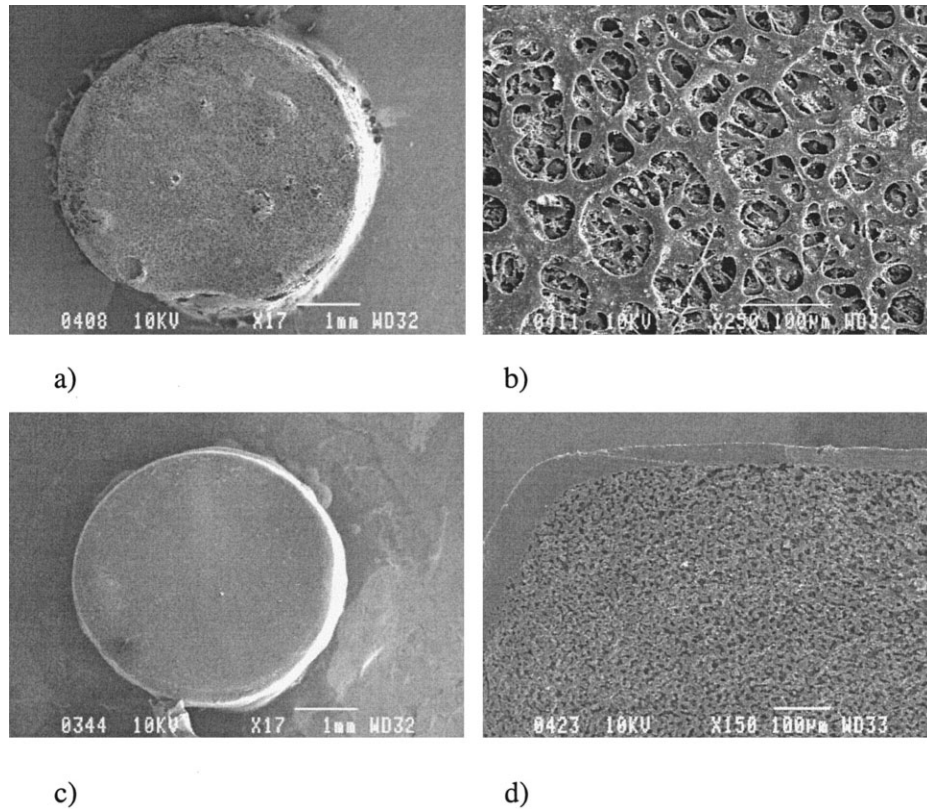


**Figure 4** SEM micrographs of disks with an open-cell asymmetric structure ((a), (b): top surface) and with a closed-cell structure ((c): top surface; (d): inside lateral section).

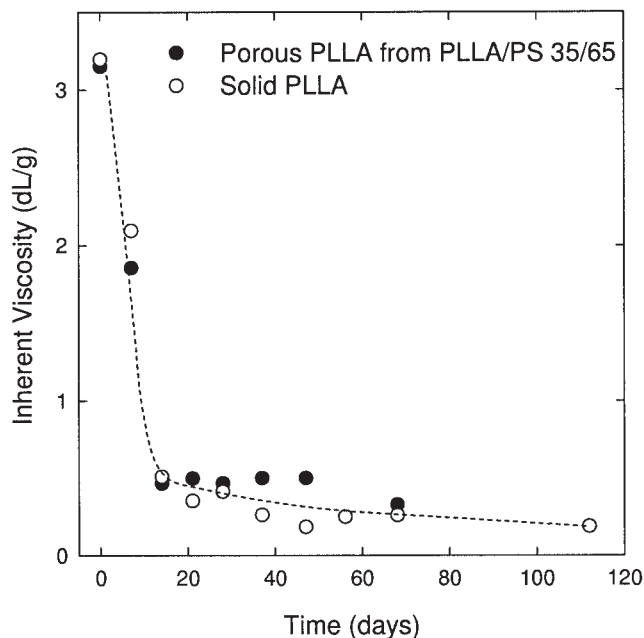


**Figure 5** Inherent viscosity of solubilized PLLA from 65% porous PLLA and the 100% PLLA control disks subjected to accelerated *in vitro* degradation.

porous disks. After 16 weeks, the remaining weight is about 40 and 15% of the initial weight for the nonporous and the porous material, respectively. Note that some experimental uncertainty may result related to the experimental difficulty of recovering the smaller particles by filtration in the case of the porous disk, but this effect is considered to be minor. For the same initial disk volume, one should remember that the weight of the porous disk (~65% porous) was about 35% of the weight of the nonporous disk. Thus, these experiments indicate that the absolute value of the remaining weight of the porous structure is more than seven times lower than that of the nonporous material, after 16 weeks of *in vitro* degradation. Clearly, the large increase of the contact surface area between the polymer and the solution leads to an increased rate of degradation and this approach may be a more effective and straightforward route to enhance PLLA degradation than modifying the hydrolytic scission mechanism of degradation itself.

#### Compressive mechanical properties

Compressive tests were carried out on 50% void volume cylinders of fully-interconnected porosity, pre-



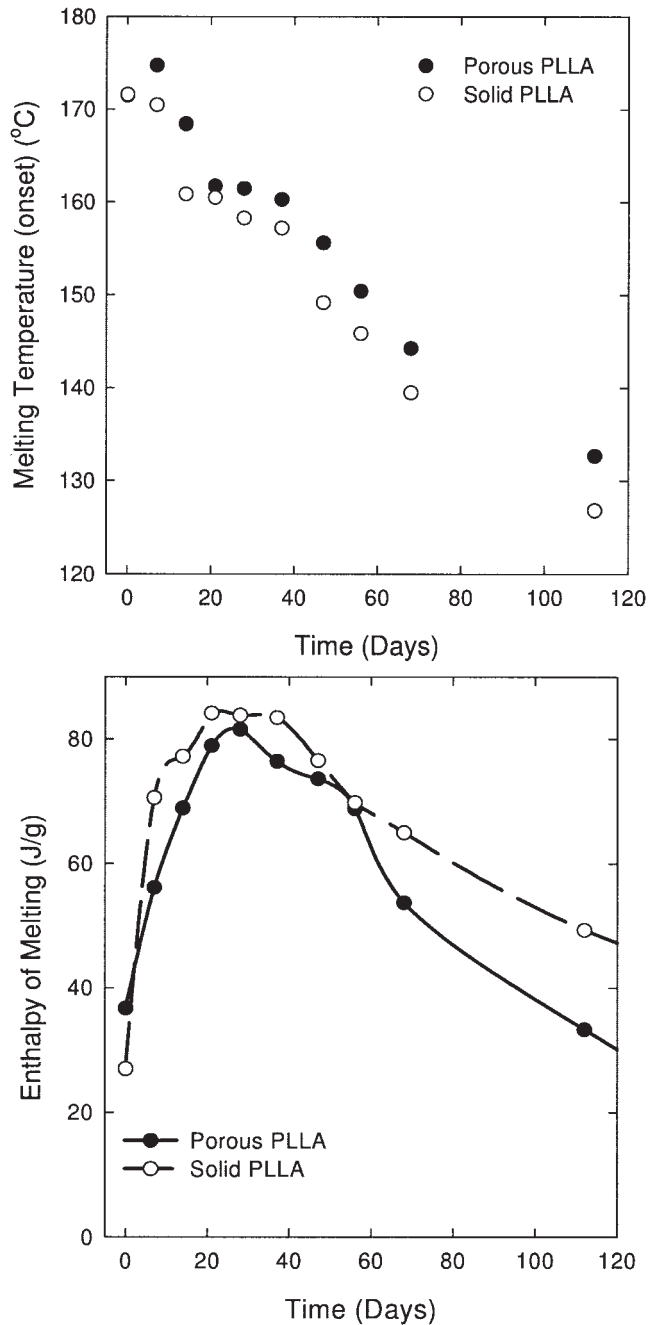


Figure 6 Melting temperature and enthalpy of melting, estimated by DSC, for 65% porous PLLA and solid PLLA disks subjected to accelerated *in vitro* degradation.

pared as outlined in the experimental. Cylinders with a closed-cell external surface were prepared for three wall thicknesses (example in Fig. 8), while others were hollowed out to obtain tubes of three thicknesses (Fig. 9). The compressive strength is taken in the plateau region at 10% strain. The compressive strength and modulus for the nonporous solid cylinders is found to be about 100 MPa (maximal strength instead of the strength at 10% strain) and 2000 MPa, respectively.<sup>16</sup>

Although the standard deviation for the porous samples is found to be  $\pm 5$  to  $\pm 10\%$  for the strength and from  $\pm 1.5$  to  $\pm 13\%$  from the modulus, the average values reported in Figures 10 and 11 show distinct tendencies. Figure 10 indicates that the properties for porous PLLA are lower, but they can be improved when an external closed-cell wall is present. Closed-cell structural articles can have essentially the same external surface as the nonporous articles. Note that the wall thickness was measured from SEM micrographs and represents the average of five measurements. Figure 11 indicates that the properties for the tubes of 500  $\mu\text{m}$  to 1 mm thickness are also close to those of the original porous PLLA cylinder. It is clearly demonstrated that both closed-cell and tubular type porous structures can be designed to acquire particular mechanical properties. These materials are more elastic than the nonporous solid PLLA, and demonstrate a compressive behavior similar to foams. Such porous structures could be used when a moderate modulus in compression is required. The addition of hydroxyapatite particles in the initial blend could also be an interesting approach to increase the mechanical properties.

CONCLUSIONS

A procedure is presented to prepare porous PLLA disks or cylinders from polymer blends with a interconnected porosity of 50 or 65% void volume. It is

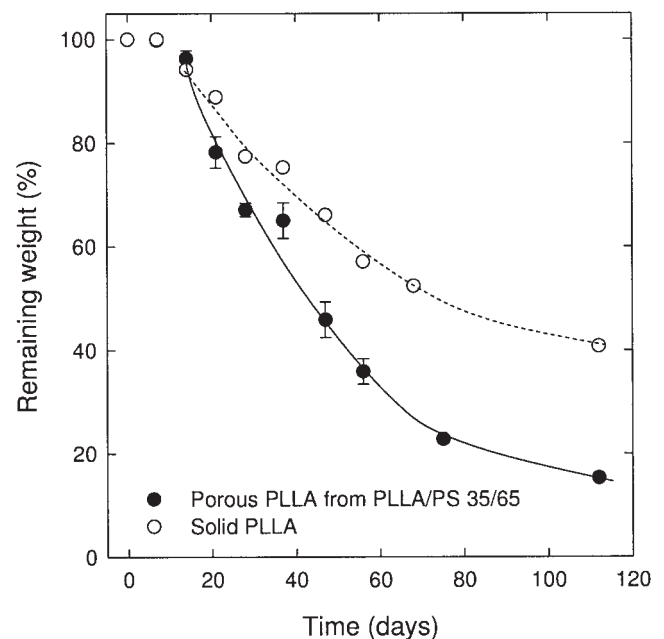
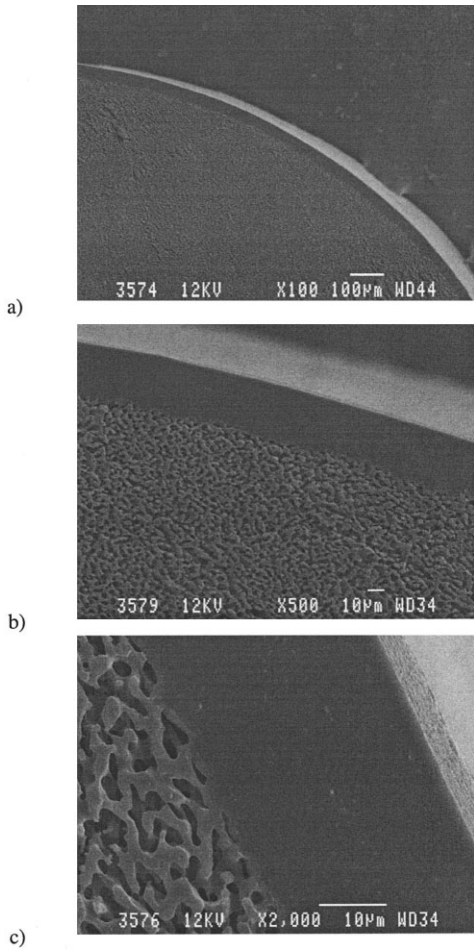
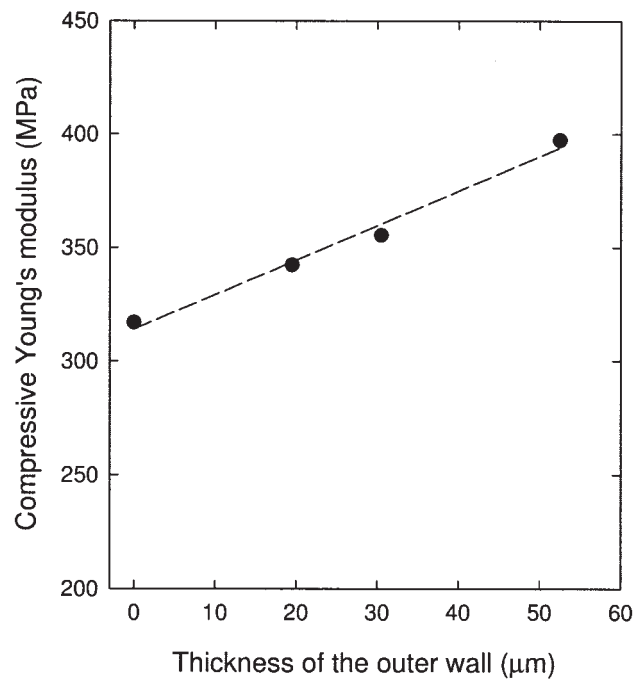
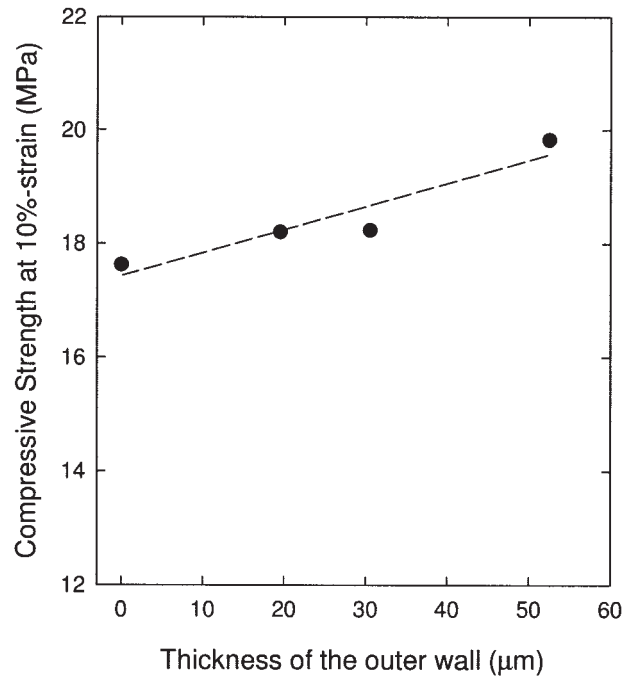


Figure 7 Evolution of the remaining percent weight after drying during the degradation test.



**Figure 8** SEM micrographs of parts of cylinders with a closed-cell structure of controlled thickness prepared from a PLLA/PS 50/50 blend: (a)  $\times 100$  magnification; (b)  $\times 500$  magnification; (c)  $\times 2000$  magnification.



**Figure 10** Compressive Young's modulus and strength at 10% strain as a function of the thickness of the nonporous outer wall.

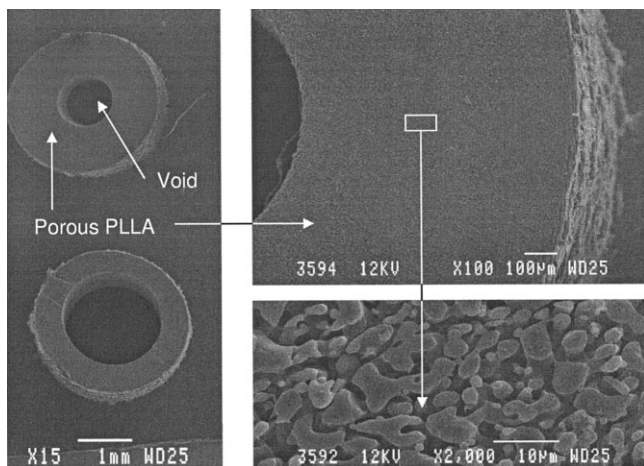


**Figure 9** SEM micrographs of porous PLLA hollow-center tubes.

demonstrated that such materials represent a viable alternative to nonporous degradable biomaterials since it is possible to modulate the degradation and the mechanical properties. The accelerated *in vitro* degradation for porous and nonporous PLLA disks indicates a similar behavior for the melting tempera-



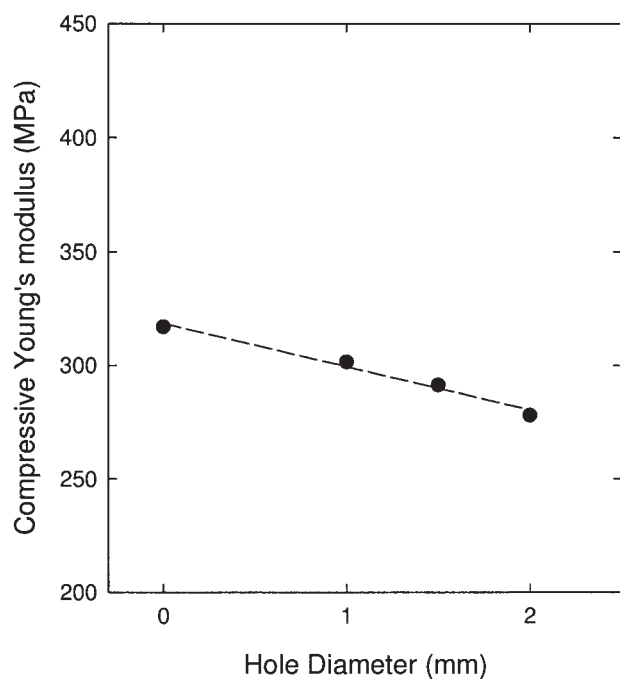
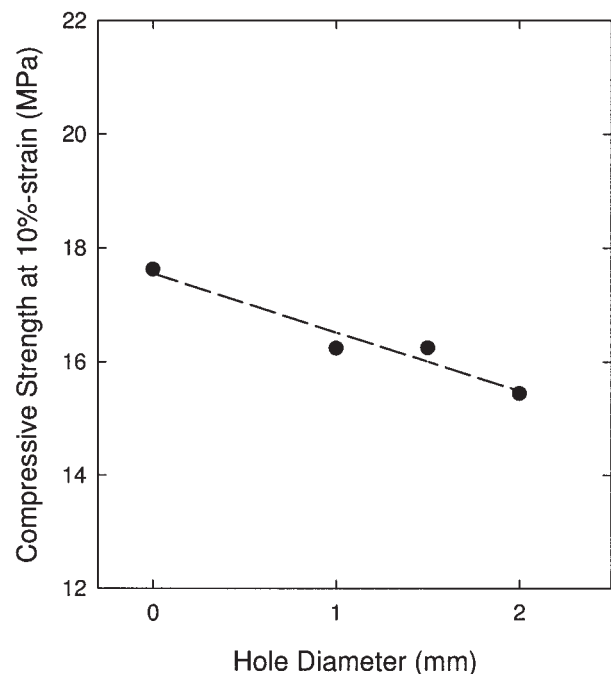


**Figure 11** Compressive Young's modulus and strength at 10% strain as a function of the hollow tube diameter inside the cylinder.

ture and the inherent viscosity of the degraded specimens, but the crystallinity and the residual are much smaller for the porous specimens. The *in vitro* degradation experiments indicate that the absolute value of the remaining weight of the porous PLLA structure is more than seven times lower than that of the nonporous material, after 16 weeks of degradation. The mechanical properties under compression, measured for open cell, closed cell, and tubular porous structures were compared with nonporous PLLA, and the results demonstrate the high mechanical integrity of such structures. In addition to a highly sophisticated level of porous morphology control, another advantage of this approach is that it can be used to fabricate porous materials over a wide range of sizes and geometrical shapes.

P. Sarazin expresses appreciation to the Province of Québec for a postgraduate scholarship from the Fonds de Recherche sur la Nature et les Technologies (FQRNT).

## References

1. Maquet, V.; Jerome, R. *Mater Sci Forum* 1997, 250, 15.
2. Peters, M. C.; Mooney, D. J. *Mater Sci forum* 1997, 250, 43.
3. Böstman, O.; Pihlajamäki, H. *Biomaterials* 2000, 21, 2615.
4. Furukawa, T.; Matsusue, Y.; Yasunaga, T.; Shikinami, Y.; Okuno, M.; Nakamura, T. *Biomaterials* 2000, 21, 889.
5. Durucan, C.; Brown, P. W. *Adv Eng Mater* 2001, 3, 227.
6. Vert, M.; Li, S. M.; Spenlehauer, G.; Guerin, P. *J Mater Sci: Mater Med* 1992, 3, 432.
7. van der Elst, M.; Klein, C. P. A. T.; de Blicq-Hogervorst, J. M.; Patka, P.; Haarman, H. J. T. M. *Biomaterials* 1999, 20, 121.
8. Laitinen, O.; Pihlajamäki, H.; Sukura, A.; Böstman, O. *J Biomed Mater Res* 2002, 61, 33.
9. Sarazin, P.; Favis, B. D. *Biomacromolecules* 2003, 4, 1669.
10. Favis, B. D.; Sarazin, P.; Li, J.; Yuan, Z. Microporous articles comprising biodegradable medical polymers, method of preparation thereof and method of use thereof. U.S. Pat. (submitted).
11. Dunne, M.; Corrigan, O. I.; Ramtoola, Z. *Biomaterials* 2000, 21, 1659.
12. Holy, C. E.; Cheng, C.; Davies, J. E.; Shoichet, M. S. *Biomaterials* 2001, 22, 25.
13. ISO Standard 13781, 1997.
14. Tsuji, H.; Ikarashi, K.; Fukuda, N. *Polym Degrad Stab* 2004, 84, 515.
15. Washburn, E. W. *Phys Rev* 1921, 17, 273.
16. Sarazin, P.; Roy, X.; Favis, B. D. *Biomaterials* 2004, 25, 5965.